BIOCHEMISTRY
including biophysical chemistry & molecular biology

Article

pubs.acs.org/biochemistry

Structural Evolution and Membrane Interaction of the 40-Residue β Amyloid Peptides: Differences in the Initial Proximity between Peptides and the Membrane Bilayer Studied by Solid-State Nuclear Magnetic Resonance Spectroscopy

Wei Qiang,* Rumonat D. Akinlolu, Mimi Nam, and Nicolas Shu

Department of Chemistry, Binghamton University, State University of New York, Binghamton, New York 13902, United States

Supporting Information

ABSTRACT: Interactions between the β amyloid (Aβ) peptides and cellular membranes have severe consequences such as neuronal cell disruption and therefore may play important roles in Alzheimer's disease. Understanding the structural basis behind such interactions, however, is hindered by the complexity of the Aβ−membrane systems. In particular, because the Aβ peptides are partially incorporated in the membrane bilayer after enzymatic cleavage, there are multiple possibilities in terms of the initial proximity between the peptides and membranes. Structural studies using *in vitro* model systems with either externally added or preincorporated Aβ in membrane bilayers resulted in distinct evolution pathways. Previous work has shown that the externally added Aβ formed long and mature filaments, while preincorporated Aβ generated short and curvy fibrils. In this study, we perform detailed characterizations on the structural evolution and membrane interaction for these two pathways, using a combination of solid-state nuclear magnetic resonance spectroscopy and other techniques. For the externally added Aβ, we determined the residue-specific structural evolution during the fibrillation process. While the entire fibrillation process for the externally added Aβ was slow, the preincorporated Aβ generated Aβ−lipid complexes rapidly. Specific interactions between the lipids and peptides were observed, suggesting the colocalization of lipids and peptides within the complex. Formation of such a complex induced molecular-level changes in the lipid bilayer, which may serve as a possible mechanism of membrane disruption.

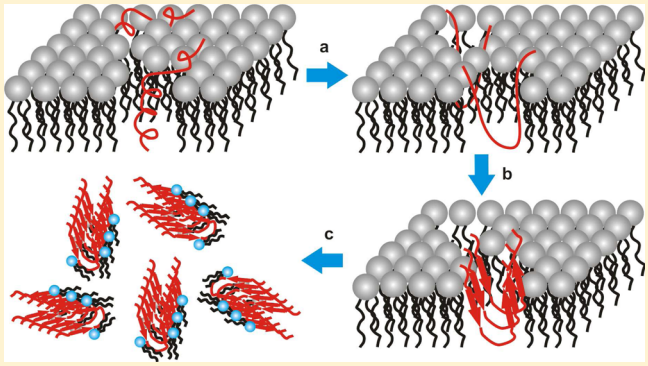

Deposition of the β amyloid (Aβ) plaques has been considered a major clinic hallmark in identifying Alzheimer's disease (AD).[1] Although the presence of amyloid plaques has been confirmed for AD patients, the intrinsic linkage between these plaques and the progression of AD remains unclear. The amyloid cascade hypothesis states that the severe clinic symptoms, such as the death of neuronal cells, are consequences of Aβ aggregation.[2] Unfortunately, the hypothesis is currently being challenged because of the failure of several amyloid-oriented drugs in clinic tests.[1,3] These drugs, although they eliminate the production of Aβ peptides and/or degrade the existing Aβ plaques, do not have sufficient effects on the progression of the disease.[3] This controversy suggested that the hypothesis itself has been re-evaluated. In particular, the linkage between the production of Aβ and downstream clinic phenomena such as the death of neuronal cells has to be understood more deeply at the molecular level. A potential mechanism for neuronal cell toxicity of Aβ is the aggregation-induced cellular membrane disruption.[4,5] This hypothesis was supported by a number of experimental findings. First, the Aβ peptides are naturally associated with the membrane bilayer. The enzymatic cleavage sites of amyloid precursor protein (APP) that are responsible for the release of Aβ are located in the interior of membrane bilayer.[6] According to a recent structural study of the membrane-associated domain of APP, the Aβ sequence inserts partially into the phospholipid bilayer.[7,8] The isolated Aβ peptides may locate either inside or outside of the membrane. A previous study of the Aβ location using isolated plasma membranes suggested that the peptides might be enriched in both the extracellular plaques and the lipid raft domains with a large abundance of sterols.[9] Second, the Aβ peptides have been shown to induce changes in the fluidity of membrane bilayers in a variety of systems, including synthetic phospholipid liposomes, the isolated plasma membrane, and living cells.[4,5,9−15]

Although the linkage between Aβ peptides and membrane bilayers exists naturally, there has not been a systematic characterization of the molecular interactions. The Aβ sequence is intrinsically disordered in aqueous buffer and possesses a strong aggregation tendency under physiological conditions.

Received: August 11, 2014
Revised: November 13, 2014
Published: November 14, 2014

dx.doi.org/10.1021/bi501003n | *Biochemistry* 2014, 53, 7503−7514

However, the high-resolution structures of Aβ aggregates are known to be highly sensitive to the detailed conditions used *in vitro*.[16] For instance, previous works have characterized the effects of pH values, temperature, and ionic strength on the Aβ fibril structures.[16−19] Under certain extreme conditions such as low temperatures, metastable protofibrils or spherical oligomers may also be stabilized and separated.[18] Recent studies using the Aβ fibril seeds extracted from human brain have also elucidated the molecular-level structural variations in fibrils from AD patients with different clinic histories.[20] Such findings indicated that the Aβ fibril structural variation did exist because of the variations in the biological environments in human beings, not only because of the experimental artifacts *in vitro*.

The introduction of a phospholipid bilayer provides an environment distinct from the aqueous buffer for the structural characterization of the Aβ aggregation process. The Aβ peptides were known to bind to membrane bilayers, and the binding affinities increased with a larger population of phospholipids with negatively charged headgroups.[21] Further structural evolution of Aβ may be sensitive to the molar ratio between peptides and lipids, which has been suggested by previous circular dichroism (CD) spectroscopy studies.[22] At a relatively low ratio (i.e., less than 1:50), the peptide might form a partial α-helical conformation, which may further convert into the conformation that is similar to the structural motif in mature fibrils.[5,23] A recent molecular dynamics (MD) simulation has suggested that the C-terminal fragment of Aβ had a strong tendency to form helical conformation and might insert into the bilayer interiors.[24,25] The initial proximity between Aβ and the membrane bilayer also affected the further evolution of Aβ significantly. For the Aβ peptides that were preincorporated into membrane bilayers, there have been multiple evolution pathways, including the formation of ionic channel and/or membrane pores,[26−29] the growth of fibrils with phospholipid uptake,[30] and the induction of interdigitation and asymmetry in the lipid bilayer by carpeting models.[4] Low-resolution structural evidence or imaging data that supported these Aβ evolution pathways have been obtained using a variety of techniques. For instance, the formation of an ion channel was observed using atomic force microscopy (AFM), and the selective Ca^{2+} conductance was verified using electrophysiological assays.[28] Colocalization of Aβ fibrils and phospholipids was observed by confocal fluorescence microscopy, which indicated the uptake of lipids during the fibrillation process.[22] Recently, there has been a solid-state nuclear magnetic resonance (NMR) spectroscopy study of the externally added Aβ in the membrane bilayer. The structural models obtained from multidimensional NMR spectroscopy for the membrane-associated Aβ fibrils were remarkably different from those of the fibrils obtained in the absence of a membrane.[31] However, there has been few high-resolution structural data about the Aβ−membrane interactions along different membrane disruption pathways. An important question to be answered is whether the interaction involves specific residues on Aβ. The answer will provide insights into the molecular mechanism of membrane disruption induced by Aβ amyloidosis, which has been considered as a crucial pathological mechanism for AD. In addition, information about the specific Aβ−membrane interaction allows the design of inhibitors.[32−34] For the externally existed Aβ peptides, there have been studies shown that they may form fibrils more rapidly, presumably because of the increasing local peptide concentrations on the bilayer surface.[5] Importantly, Aβ can be located either inside or outside of membrane bilayers because of the initial partial insertion configuration after cleavage. Simultaneously, the detailed mechanisms for Aβ release and cleaning remain unclear,[35] which means both initial proximities will have to be considered for *in vitro* studies.

We have previously investigated the evolution pathways of Aβ located both inside and outside of phospholipid bilayers.[36] The transmission electron microscopy (TEM) results suggested distinct time-dependent morphological evolutions for samples prepared with either externally added or preincorporated Aβ. While the externally added Aβ formed mature and straight fibrils over a long incubation time period, the fibrils produced by preincorporated Aβ remained short (i.e., a few hundred nanometers) and curvy after incubation for 14 days. In this work, we focus on the high-resolution structural details under both circumstances. Using solid-state NMR spectroscopy, we monitored the residue-specific structural evolution of the externally added Aβ and obtained information about structural convergence along with the fibrillation process. For the preincorporated Aβ, we detected specific contacts between certain amino acids and phospholipids, which suggested the formation of complexes between Aβ aggregates and lipids. In addition, the formation of such a complex may be accompanied by a change in the integrity of membrane disruption, which provides a possible mechanism for membrane disruption.

MATERIALS AND METHODS

Peptide Synthesis and Purification. All peptides (with the same DAEFRHDSGYEVHHQKLVFFAEDVGSNKGAIIG-LMVGGVV primary sequence) were synthesized using 9-fluorenylmethyloxycarbonyl chloride (FMOC) chemistry on a 433A peptide synthesizer (Applied Biosystems, Inc., Foster City, CA) using a low-substitution Fmoc-Val-Wang resin (0.3 mmol/g, AAPPTec, LLC, Louisville, KY) and purified using an Agilent high-performance liquid chromatography (HPLC) system (HP 1100 Series, Agilent Technologies, Inc., Santa Clara, CA) equipped with a C18 reversed-phase semi-preparative column (Zorbax C-18, Agilent Technologies, Inc.). The linear water−acetonitrile gradient was used for the HPLC purification, and the purities of all products were identified using matrix-assisted laser desorption ionization time-of-flight mass spectrometry (MALDI-TOF-MS) (Applied Biosystems, Inc.). Uniformly ^{13}C- and ^{15}N-labeled amino acids (Cambridge Isotope Laboratory Inc., Tewksbury, MA) were incorporated into the peptide sequences for the synthesis of the isotope-labeled peptides.

Preparation of Liposome Samples. Liposome samples were prepared with externally added Aβ peptides or via the preincorporation of Aβ peptides, using similar protocols from our previous work.[36] All phospholipids were purchased from Avanti Polar Lipids, Inc. (Alabaster, AL), and cholesterol was obtained from Sigma-Aldrich (St. Louis, MO). For the external addition samples, the mixture of phospholipids and/or cholesterol in chloroform was dried with an Ar flow, followed by overnight vacuum dehydration. The lipid film was resuspended in 10 mM phosphate buffer (pH 7.4, with 0.01% NaN_3) to achieve a final lipid concentration of 1.5 mM. The liposome solution was allowed rotate at ambient temperature for 1 h with occasional bath soncation and extruded through a 200 nm pore size polycarbonate membrane (Avanti Polar Lipids, Inc.). Freshly dissolved Aβ peptides in dimethyl sulfoxide were then added to the liposome solution with vigorous vortexing to ensure thorough mixing, and the final

peptide concentration was 50 μM. For the preincorporated samples, the lipid/cholesterol mixture in chloroform was mixed with the designed amount of Aβ peptides in trifluoroacetic acid (TFA). The mixture was dried with Ar and high vacuum, resuspended in phosphate buffer, and extruded as described above. Previous studies have shown that Aβ will not form fibrils in phosphate buffer at a concentration of 50 μM in 1 h.[37] The Aβ–liposome mixtures were then allowed to incubate quiescently at 37 °C until further measurements were taken.

Fluorescence Measurements. Two types of fluorescence assays were performed in this work, and both of them were conducted on a PerkinElmer (Waltham, MA) LS55 fluorophotometer with temperature control using a circulated water bath. For the thioflavin T (ThT) measurements of fibril growth kinetics, a 100 μL aliquot of the Aβ–liposome solution was mixed with 5 μL of a 4 mM ThT solution. The fluorescence cuvette was capped and sealed using parafilm to prevent evaporation during the measurements. Fluorescence emission at 490 nm was recorded continuously for 4 h with an excitation wavelength of 440 nm and a 5.0 s interval between the adjacent data point, and the excitation and emission slits were both set to 5.0 nm. For the lipid mixing assay, the solution contained 20% fluorophore-labeled liposomes, which had 1 mol % 1,2-dipalmitoyl-*sn*-glycero-3-phosphoethanolamine-*N*-(7-nitro-2-1,3-benzoxadiazol-4-yl) (NBD-PE) and 1 mol % 1,2-dipalmitoyl-*sn*-glycero-3-phosphoethanolamine-*N*-(lissamine rhodamine B sulfonyl) (Rh-PE) (Avanti Polar Lipids, Inc.) relative to the total lipids. Fluorescence emission at 585 nm was recorded for the same time period as the ThT measurement with an excitation wavelength of 470 nm. The excitation and emission wavelengths were chosen to detect the fluorescence resonance transfer between the two fluorophores.[38,39]

Circular Dichroism (CD) Spectroscopy. CD spectroscopy was applied to the preincorporated samples to track the global structural evolution during the initial stage of incubation. An Aβ–liposome solution (12 μL) was taken from the incubated sample at different time points and mixed with 288 μL of deionized water. The original solution was diluted to prevent any further structural evolution during the measurements. The CD spectra were recorded on a JASCO (Easton, MD) J-810 spectrometer with the temperature at 20 °C. The spectrum for each sample was recorded from 190 to 260 nm with signal averaging over 40 scans. The background spectrum was recorded using only liposomes in the absence of peptides and subtracted from the spectra of the sample solution. Data fitting of the CD spectra was performed using CDPro.[40]

Solid-State NMR Spectroscopy. Samples for NMR measurements were prepared by ultracentrifugation at 432000*g* for 1 h at 4 °C (Beckman Coulter Inc., Pasadena, CA). The pellet was lyophilized and rehydrated with deionized water (1 μL of H_2O/mg of sample) after being packed into the 2.5 mm magic angle spinning (MAS) rotors. All NMR experiments were performed on a 600 MHz Bruker Avance III spectrometer (Bruker Biosciences Corp., Billerica, MA) equipped with a 2.5 mm HXY TriGamma MAS probe. All samples were maintained at ambient temperature using a N_2 flow throughout the experiments. The static and MAS ^{31}P spectra were recorded using a direct polarization radio-frequency (rf) pulse at ~50 kHz with ~100 kHz ^{1}H continuous-wave (CW) decoupling. The T_2 relaxation measurements were taken using a Hahn spin echo pulse sequence, which included ~50 kHz ^{31}P rf pulses and ~100 kHz ^{1}H CW decoupling. Two-dimensional (2D) ^{13}C–^{13}C correlation spectra were recorded with 10 and 500 ms radiofrequency-assisted diffusion (RAD) mixing periods for the detection of intraresidue and long-range cross-peaks, respectively.[41] The RAD pulse sequence also contained ~60 kHz ^{1}H cross-polarization (CP) block and 40–56 kHz ^{13}C CP over 1.5 ms, and 100 kHz two-pulse phase modulation (TPPM) ^{1}H decoupling. The one-dimensional (1D) ^{13}C–^{31}P rotational echo double resonance (REDOR) spectra were recorded with a 18 ms dephasing period, which detected ^{13}C–^{31}P distances of roughly $\leq$7 Å.[42] The difference spectra were obtained by subtracting the time domain signal of S_1 (with the ^{31}P π pulses on) from that of S_0 (with the ^{31}P π pulses off) followed by Fourier transformation. Both the 2D RAD and REDOR experiments were performed with a 10 kHz MAS frequency. 1D PITHIRDs-CT experiments were conducted with 20 kHz MAS frequency and 16.7 μs ^{13}C π pulses.[43] The constant time period was kept at 31.2 ms, while the effective dephasing time varied from 0 to 31.2 ms with an interval of 2.4 ms. The ^{1}H decoupling fields were kept at 100 kHz during the constant time period and 75 kHz during the acquisition time. Numerical simulation for the ^{13}C PITHIRDs decay curve was conducted using the SIMPSON simulation package and a model spin system of five equally spaced ^{13}C nuclei.[44] The 2D spectra with 10 and 500 ms mixing periods were acquired with signal averaging for 24 and 48 h, respectively. All 2D spectra were processed with 120 Hz Gaussian line broadening in both dimensions.

RESULTS

^{31}P NMR Reveals Perturbation of Membranes by Preincorporated Aβ. Our previous TEM studies have shown that for the preincorporated Aβ samples, there seemed to be fragmentized vesicles within a short incubation time. On the other hand, the overall morphology of liposomes remained intact for the externally added samples.[36] In addition, the previous work included ^{31}P solid-state NMR spectra on Aβ/POPC liposomes under the two sample preparation conditions.[36] To further investigate any possible membrane perturbation, we measured the ^{31}P chemical shift anisotropy (CSA), the isotropic ^{31}P chemical shifts, and the ^{31}P spin–spin (T_2) relaxation time constants for the preincorporated Aβ in 100% POPC liposomes, 80% POPC/20% POPG liposomes, and 80% POPC/20% POPG liposomes with additional 30% cholesterol (30% relative to the total mass of lipids). These membrane compositions were chosen to study the effects of negatively charged phospholipids and cholesterol on Aβ–membrane interactions, both of which have been proposed to be important.[7,8,21,45,46] For each sample, ^{31}P NMR spectra were recorded at 0, 1, and 4 h incubation time periods because previous TEM images showed significant fragmentation within 4 h. Figure 1 shows the plots of time-dependent ^{31}P signal decay caused by T_2 relaxation for different samples, measured using a Hahn echo pulse sequence under MAS. Representative static and MAS ^{31}P spectra are provided in the Supporting Information. Additional parameters such as ^{31}P CSA, isotropic chemical shift, and fitting of the T_2 constant are provided in Table 1. The overall construct of the liposome seemed not to be affected, as there was little change in either the line shape of the static ^{31}P spectra or the isotropic chemical shifts. However, the ^{31}P relaxation time constant became shorter for the POPC/POPG sample as the sample was incubated for 4 h. Changes in ^{31}P T_2 indicated the low-frequency motion of phospholipids and the diffusion of lipids in bilayers.[47] The decrease in the T_2

dx.doi.org/10.1021/bi501003n | *Biochemistry* 2014, 53, 7503–7514

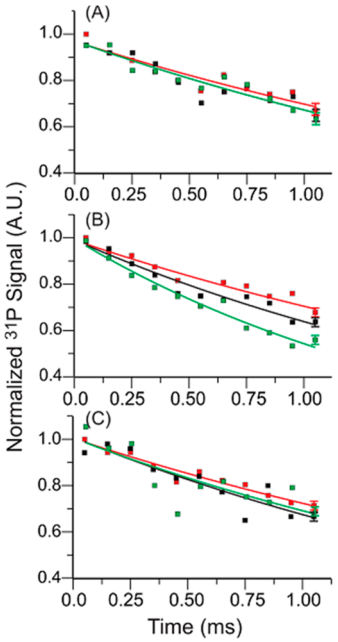

Figure 1. Plots of ^{31}P T_2 relaxation for the preincorporated samples with (A) POPC, (B) POPC/POPG, and (C) POPC/POPG/cholesterol liposomes. For each sample, data were collected at different incubation time periods: starting point (red), incubation for 1 h (black), and incubation for 4 h (green). Each data set was fit to a single-exponential decay function to obtain the relaxation time constant, and the best-fit results are provided in Table 1. The size of error bars reflects the noise level in each set of decay, which was estimated from the experimental spectral noise.

Table 1. Structural Parameters Derived from ^{31}P Solid-State NMR Experiments on Preincorporated Aβ−Liposome Samples

lipids[a]	time (h)	CSA (ppm)[b]	ICS (ppm)[c]	T_2 (ms)
PC	0	48.0	−2.1	3.04(0.38)
	1	53.0	−2.1	2.86(0.38)
	4	40.0	−2.1	2.87(0.32)
PC/PG	0	47.6	−2.1, −3.3[d]	2.94(0.34)
	1	43.8	−2.1, −3.5	2.32(0.19)
	4	43.0	−2.0, −3.7	1.68(0.11)
PC/PG/Chol	0	47.1	−2.1, −3.4	3.06(0.24)
	1	43.3	−2.1, −3.3	2.66(0.40)
	4	40.4	−2.2, −3.8	2.50(0.60)

[a]The compositions of lipids used in liposomes. PC, PC/PG, and PC/PG/Chol stand for 100% POPC liposomes, 80% POPC/20% POPG liposomes, and 80% POPC/20% POPG liposomes with additional 30 mol % cholesterol, respectively. [b]CSA, or the ^{31}P chemical shift anisotropy, was detected using static ^{31}P NMR spectroscopy. [c]The isotropic chemical shift was detected using MAS ^{31}P NMR spectroscopy. [d]The two chemical shifts were assigned to ^{31}P located in POPC and POPG, respectively.

relaxation time upon incubation with preincorporated Aβ suggested an increase in the level of lipid motion and a possible destabilization of the membrane bilayer.[48] The increase in the ^{31}P relaxation rate has been observed only for liposomes with negatively charged lipids, while the absence of this component or the presence of 30 mol % cholesterol eliminated the effect. Furthermore, certain decay curves (e.g., the sample with cholesterol at 4 h) did not fit well to the exponential function, and this deviation seemed not to be a consequence of a high level of spectral noise.

Fluorescence Measurements Suggested Lipid Uptake with Aβ Aggregation. We further investigated the time-dependent interactions between Aβ and the membrane in both external addition and preincorporation circumstances using fluorescence spectroscopy. The time-dependent ThT fluorescence emission and lipid mixing were recorded for the first 4 h of the incubation period for the POPC/POPG liposomes. Figure 2 showed that there was a rapid buildup in the ThT

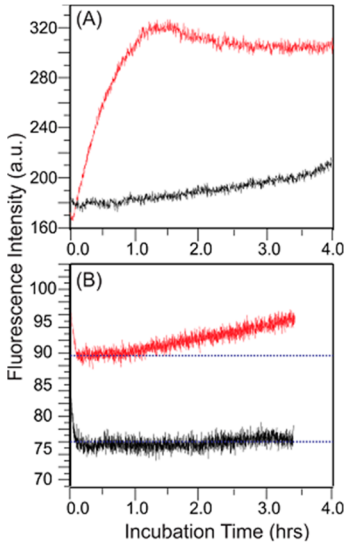

Figure 2. (A) ThT fluorescence emission intensities recorded at 490 nm for externally added (black) and preincorporated (red) sample preparation methods with POPC/POPG liposomes. Fluorescence intensities were recorded continuously for 4 h. (B) Lipid mixing assay using liposomes labeled with NBD-PE and Rh-PE. Fluorescence emission was recorded at 585 nm, corresponding to the emission wavelength of Rh-PE. Data for the externally added and preincorporated sample conditions are colored black and red, respectively. The increment in the emission intensity indicated the shorter distance between the two fluorophores. Both experiments were conducted at 37 °C, using a fluorimeter with a circulated water temperature controller.

fluorescence for the preincorporated samples, while the increase was much slower for the external addition samples. This is consistent with the measurements in our previous work in which separated data points were taken at different incubation times.[36] However, previous measurements have shown that for the preincorporated samples, it was generally true that the ThT fluorescence reached a plateau after ∼30 h, while here the fluorescence seemed to level off after incubation for 1 h. We recorded ThT fluorescence intensities at later incubation times and observed that there seemed to be a discrete increase in fluorescence. Similar phenomena have also observed by studies of Aβ fibrillation by other groups.[49] More interestingly, the time-synchronized lipid mixing assay showed that there was an increased fluorescence emission for the preincorporated sample, but not the external addition one. The assay measured the fluorescence transfer between two fluorophore-labeled lipids, which was dependent on the dipolar coupling strength between the two fluorophores. Increments in the emission intensity indicated either a shorter distance or less dynamics, which provided stronger dipolar coupling. Considering both the fluorescence and the ^{31}P measurements, it is possible that a fraction of the lipids is involved in a rigid

dx.doi.org/10.1021/bi501003n | Biochemistry 2014, 53, 7503−7514

structure during the initial incubation of preincorporated Aβ with POPC/POPG liposomes. We noticed that the rapid increase in ThT fluorescence reached its plateau at ~1 h, while the enhancement of the fluorescence signal in the lipid mixing assay started after 1 h. It was possible that the species with a high ThT fluorescence was also responsible for the lipid mixing. It was proposed previously for the membrane-associated islet polypeptide (IAPP) that the fibril growth could induce lipid uptake by cofibrillation between the peptide and lipids.[30] The same mechanism might also be involved in this case where the rapidly formed species contains a complex of Aβ and phospholipids.

CD Spectroscopy Revealed Rapid Formation of the β-Strand Conformation. We utilized CD spectroscopy to monitor the evolution of global secondary structures of Aβ in the preincorporated POPC/POPG liposome (i.e., Figure 3).

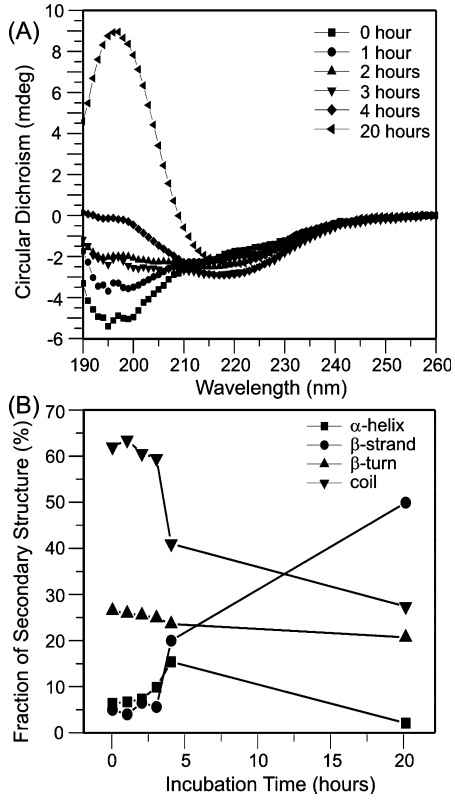

Figure 3. (A) CD spectra for a preincorporated sample with POPC/POPG liposomes at different incubation times. (B) Plots of the population of different secondary structures as a function of incubation time based on the fitting of the individual CD spectrum using CDPro.

The strong positive absorption at <200 nm and the negative CD peak at ~216 nm indicated the formation of the β-strand conformation. Fitting of the CD spectra showed that the fraction of β-strand increased from ~5 to ~20% within 4 h, and the trend of increases continued. Using our previously published TEM results in which the curvy fibrillar morphologies were observed at 4 h, we concluded that certain Aβ aggregates formed rapidly.

2D Correlation Spectroscopy Suggested Different Structural Convergence Rates for Externally Added and Preincorporated Samples. To further investigate the high-resolution structural features of the evolution of membrane-associated Aβ, we applied solid-state NMR spectroscopy to both the externally added and preincorporated samples. The liposomes were composed of a mixture of POPC and POPG at a 4:1 molar ratio, because it has been shown that the most significant changes occurred upon Aβ association in the ^{31}P relaxation measurements. Panels A and B of Figure 4 display series of 2D ^{13}C−^{13}C correlation spectra acquired at different time points during the fibrillation process of the externally added samples. Two isotope-labeled peptides were studied with uniform ^{13}C labeling at F19, A21, D23, S26, K28, A30, L34, and V40. These sites were chosen to cover the N- and C-terminal β-strands as well as the loop region between strands based on the known fibril structures.[16−20,50] Overall, the structural convergence was observed after incubation for 1 week, as indicated by a main set of chemical shifts for each amino acid. However, different labeled sites might have different structural convergence rates. For instance, the cross-peaks for A30 and L34 did not show obvious change after incubation for 2 days, which suggested that these two sites formed well-ordered structure most rapidly. In all previously published Aβ fibril structures, these residues were located in the center of the hydrophobic core, with their side chains forming the steric zipper. Residues D23 and S26 have shown time-dependent chemical shift evolution. These two residues were located in the loop region, and their conformations might be more flexible at the initial stage of fibrillation. Residues K28 and V40 have shown a weak signal over the entire incubation time, which indicated a disordered conformation in these two sites. V40 was located at the C-terminus, so its conformational flexibility was expected. In previously published Aβ fibril structures, the side chain of K28 could adopt multiple possible orientations, depending on how the positive charge was compensated.[16−20] Panels C and D of Figure 4 showed the 2D spectra for preincorporated Aβ samples with the labeling schemes. Surprisingly, at the same initial Aβ concentration (i.e., 50 μM) and peptide:lipid molar ratio (i.e., 1:30), the preincorporated samples have exhibited structural homogeneity much more rapidly. There was only one set of chemical shifts for all labeled sites during the 4 h incubation. This is consistent with the TEM observation in which the curvy fibrils started to form in 4 h and the curvy morphology remained the same after long incubation periods.[36] As shown in Table 2, differences in chemical shifts were observed between the externally added and preincorporated samples, and the magnitude of chemical shift differences varied between residues from 0.6 to 2.3 ppm for the backbone Cα atoms. The results suggest that the fibrils formed under these two sample preparation conditions had distinct core structures.

Long-Range Interactions between Aβ and Lipids Detected by NMR. We applied multiple solid-state NMR techniques to investigate the high-resolution structural features of the preincorporated Aβ fibrils that were formed within a short incubation period. In particular, we attempted to obtain structural evidence to validate the formation of a complex between Aβ and phospholipids. Panels A and B of Figure 5 show the 2D ^{13}C−^{13}C spin diffusion spectra with a 500 ms mixing period. With such a long mixing time, one would expect to detect cross-peaks between two ^{13}C nuclei that are located within roughly 7−8 Å.[41,51] Cross-peaks between residues D23 and S26, S26 and K28, D23 and K28, and F19 and L34 were observed, which suggested the formation of the typical β-loop-β motif as in the commonly observed Aβ fibrils. In particular, the observation of side chain contacts between F19 and L34 was consistent with a number of Aβ fibril structures, which

dx.doi.org/10.1021/bi501003n | Biochemistry 2014, 53, 7503−7514

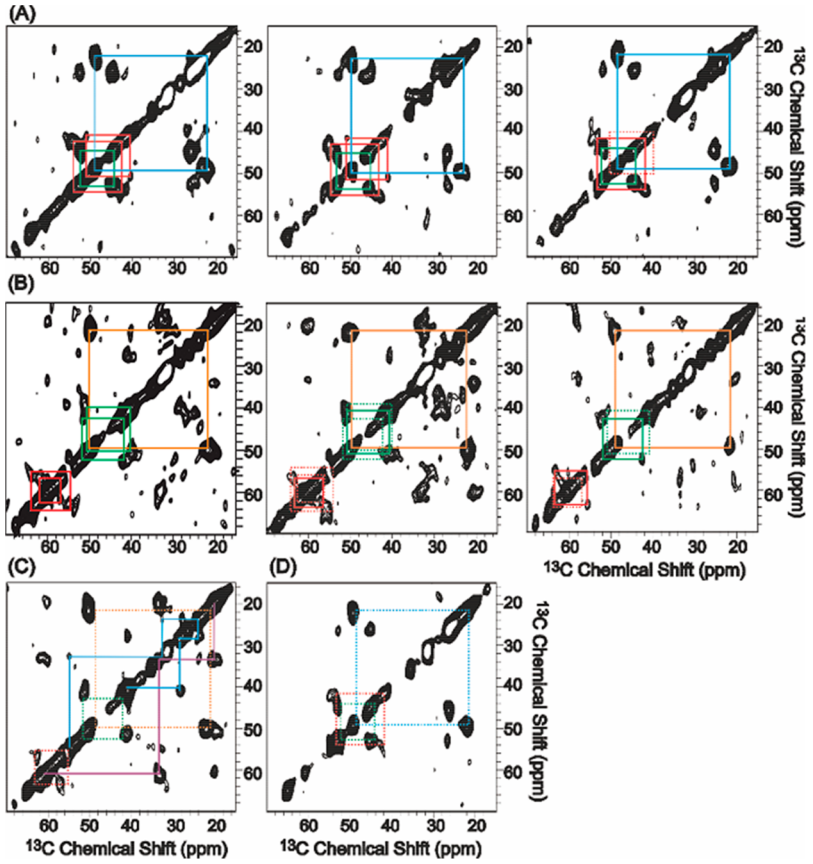

Figure 4. (A and B) 2D $^{13}C-^{13}C$ spin diffusion spectra with a short mixing time (10 ms) for the externally added Aβ sample in POPC/POPG liposomes, recorded after incubation for 2 days (left), 4 days (middle), and 8 days (right). The peptides were uniformly labeled with ^{13}C at (A) F19, A21, and L34 and (B) D23, S26, K28, A30, and V40. The C$\alpha-$Cβ cross-peaks are color-coded using a solid line rectangle as follows: (A) F19 (red), L34 (green), and A21 (cyan) and (B) S26 (red), D23 (green), and A30 (orange). For the comparison of chemical shifts between spectra with different incubation times, the positions of C$\alpha-$Cβ cross-peaks in the previous spectrum are labeled with a dotted line rectangle in the latter spectrum. In panel A, intraresidue cross-peaks were also observed between the C$\alpha-$Cγ and C$\alpha-$Cδ pairs for L34. (C and D) 2D spectra for samples with preincorporated conditions, incubation for 4 h. The dotted line rectangles indicate the cross-peak positions for the same labeling sites in the externally added samples incubated for long periods of time (i.e., 8 days), to show the difference between the fibrils obtained under these two sample preparation conditions. Two additional solid lines are shown in panel C for residues K28 (cyan) and V40 (purple). All 2D spectra were processed with 120 Hz Gaussian line broadening in each dimension. The spectra were plotted with a base-level intensity of $\sim 1.5 \times 10^4$ (arbitrary units) with an increment factor of 1.2 between the two adjacent contours. There are 64 positive contours, and the negative contours have been removed because no chemical shift information was included in the negative peaks. The typical noise level for the spectra was $\sim 0.5 \times 10^4$.

Table 2. Comparison of Chemical Shifts between the Externally Added and Preincorporated Samples

	chemical shift of externally added samples (ppm)						chemical shift of preincorporated samples (ppm)					
	Cα	Cβ	Cγ	Cδ	Cε	C′	Cα	Cβ	Cγ	Cδ	Cε	C′
F19	53.4	41.9				173.7	54.8	42.1				174.0
A21	48.8	21.7				173.0	49.4	22.0				173.5
D23	52.0	42.6				174.9	51.6	41.0				173.2
S26	55.8	63.3				174.3	57.3	62.3				173.2
K28			*a*				55.0	32.5	23.9	28.2	40.8	173.7
A30	49.2	21.7				173.8	50.1	22.0				174.0
L34	52.1	44.2	25.7			172.7	52.7	45.3	26.5			173.5
V40	57.9	33.4	21.8			178.7	60.2	33.6	20.1			179.1

[a]Cross-peaks for K28 were not observed for the externally added samples after incubation for 8 days.

indicated the packing of N- and C-terminal β-strands through the steric zipper.[16−18,20,52] Interestingly, we have also observed cross-peaks between the phospholipid methylene groups and the Cα nuclei of D23 and S26. The high-intensity peak at 31.5 ppm was assigned the bulk $(CH_2)_n$ groups in lipid acyl chains.[53] The detection of a short contact between the lipid acyl chain and specific residues in Aβ indicated that at least a fraction of lipid molecules were exposed to Aβ fibrils and were no longer located in the bilayer interiors. This result provided evidence of the formation of a complex between Aβ and phospholipids. Furthermore, it suggested that there might be specific binding sites for the lipid molecules to interact with the Aβ fibrils. We further investigated the Aβ−lipid interactions using $^{13}C-^{31}P$ rotational echo double resonance (REDOR) experiments.

dx.doi.org/10.1021/bi501003n | *Biochemistry* 2014, 53, 7503−7514

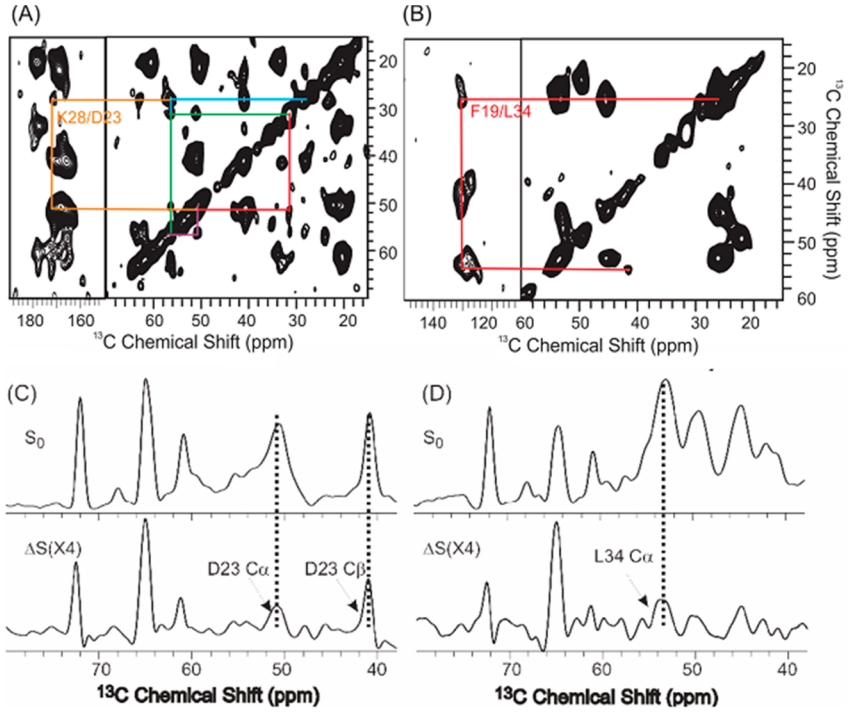

Figure 5. (A and B) 2D $^{13}C-^{13}C$ spin diffusion spectra for the preincubated samples with a 500 ms mixing period. Peptides were labeled at (A) D23, S26, K28, A30, and V40 and (B) F19, A21, and L34. In panel A, the two cross-peaks between lipid CH_2 groups and Cα atoms of D23 and S26 are colored red and green, respectively. The S26 Cα–K28 Cδ, S26 Cα–D23 Cα, and D23 Cγ–K28 Cδ inter-residue cross-peaks are colored cyan, purple, and orange, respectively. In panel B, the L34 Cγ–F19 Cζ inter-residue cross-peak is colored red. In addition, intraresidue cross-peaks were observed between the pairs of Cα and Cγ atoms and Cα and Cδ atoms for L34. (C and D) $^{13}C-^{31}P$ REDOR S_0 and ΔS spectra for the preincubated samples (POPC/POPG liposomes, incubation for 4 h). In the difference spectra, the peaks with chemical shifts of >60 ppm were attributed to lipids, and the peaks below 60 ppm were assigned to specific residues based on the 2D experiments. The 2D spectra were processed with 120 Hz Gaussian line broadening in each dimension. The spectra were plotted with a signal-to-noise ratio (SNR) of 2:1 as the lowest contour level, and 32 total contour levels with ~50% noise intensity between each level.

Panels C and D of Figure 5 displayed the REDOR full (S_0, with the ^{31}P π pulses off) and difference (ΔS) spectra with an 18 ms mixing period. This mixing time allowed detection of ~6 Å $^{13}C-^{31}P$ interactions (i.e., ~56 Hz $^{13}C-^{31}P$ dipolar coupling frequency), based on the theoretical two-spin model.[54] In the S_0 spectra, the peaks at 72.1, 67.9, 64.6, and 60.6 ppm were assigned to C_2-glycerol, β-methylene, C_1/C_3-glycerol, and α-methylene, respectively, on the basis of previous studies,[53] and the resonances between 60 and 40 ppm were attributed to Aβ. The difference spectrum with isotope labeling at D23, S26, K28, A30, and V40 showed peaks that could be assigned to C_2-glycerol, C_1/C_3-glycerol, and α-methylene from lipids, as well as Cα and Cβ from D23. For the sample with labeling at F19, A21, and L34, a weak REDOR difference peak was observed for the Cα atom of L34. Short contacts between ^{31}P and other residues in Aβ were not observed. These results indicate that the preincorporated Aβ formed a complex with specific phospholipid binding sites along the peptide backbone.

The Aβ Backbone Assembly for Preincorporated and Externally Added Samples. We applied solid-state NMR to study the backbone assembly for the complex of Aβ and lipids formed by the preincorporated samples within a 4 h incubation time. Panels A and B of Figure 6 show the ^{13}C-PITHIRDs-CT decay curves of four singly labeled sites along the Aβ sequence, as well as the simulated curves at different internuclear distances. The labeling sites, V18 C′, A21 CH_3, A30 CH_3, and M35 C′, were selected to cover both the N- and C-terminal β-strands. In general, all curves fit well to the simulated curve for an ~4.8 Å $^{13}C-^{13}C$ distance, which suggested the presence of parallel in-register β-sheet structure[55] (a cartoon model was given in the Supporting Information). In addition, the fact that all curves decay rapidly within ~30 ms suggested that there was only one population of ^{13}C structure, i.e., the parallel in-register β-sheet for the labeled sites. This result indicated that there was a rapid formation of β-sheet for the preincorporated samples. On the other hand, the backbone assembly process for the externally added Aβ samples seemed to be much slower, and residue-specific, as well. Panels C–F of Figure 6 show the ^{13}C-PITHIRDs-CT decay curves for the four labeled sites collected at different incubation times (i.e., 2, 4, and 8 days). The methyl group of A21 showed decay curves that fit well to ~5 Å after a 2 day incubation, indicating the formation of parallel β-sheet at this site with a relatively fast kinetics. Decay curves for the methyl group of A30 and the carbonyl group of M35 on day 2 were slower than those on days 4 and 8, which suggested that the C-terminal β-strands formed slower than the segment around A21. Finally, we observed that the formation of β-sheet at V18 had the slowest kinetics, where the decay curve that fit well to ~5 Å was observed only on day 8.

DISCUSSION

Extensive Solid-State NMR Studies Revealed New Structural Features for the Externally Added and Preincorporated Samples. Our previous work described preliminary biophysical and structural data on the two types of Aβ–membrane systems. The work presented here contains more extensive solid-state characterizations, with the motivation of investigating the detailed structural evolutions along

dx.doi.org/10.1021/bi501003n | Biochemistry 2014, 53, 7503–7514

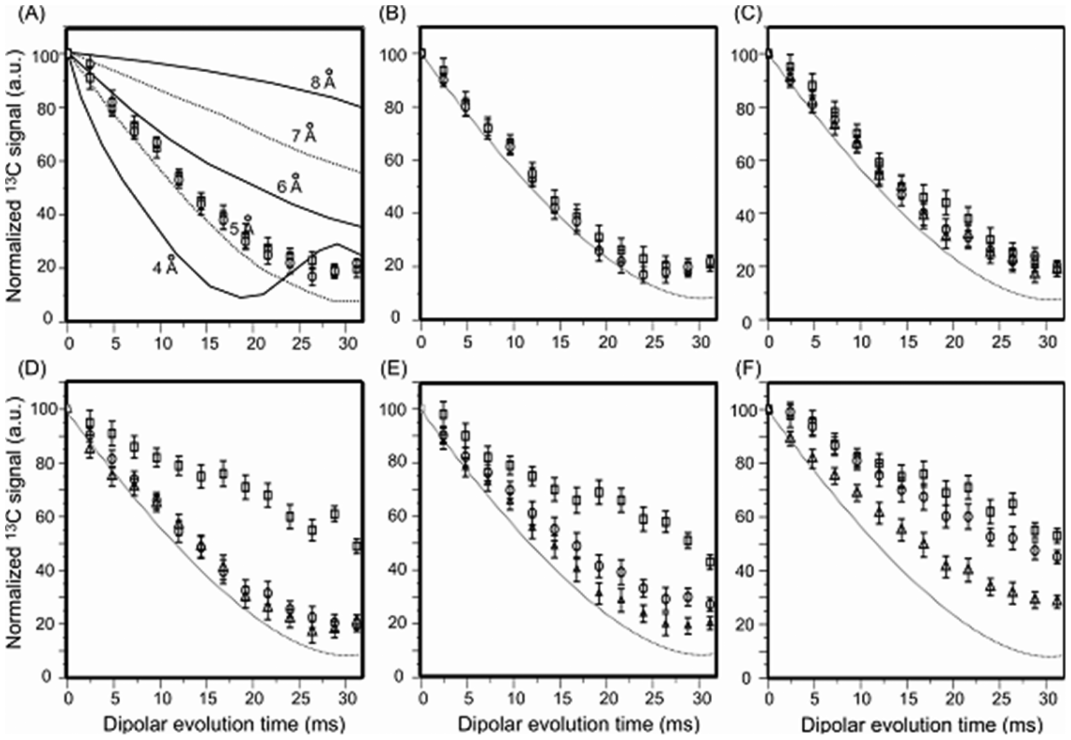

Figure 6. ^{13}C-PITHIRDs-CT decay curves for the preincorporated samples (4 h incubation time) with (A) V18 C′ (□) and A21 CH_3 (○) and (B) A30 CH_3 (□) and M35 C′ (○) and the externally added samples with (C) A21 CH_3, (D) A30 CH_3, (E) M35 C′, and (F) V18 C′. For panels C–F, the data were collected at incubation times of 2 days (□), 4 days (○), and 8 days (△). Error bars were determined from the spectral noise. Simulated ^{13}C-PITHIRDs-CT decay curves for 4–8 Å are shown in panel A, and the curves for 5 Å are provided in all panels.

different Aβ aggregation pathways. We emphasize that although the general sample preparation protocols were similar in both the previous and current work, the NMR measurements were actually performed on samples under different conditions. In particular, for the preincorporated samples, the previous data were collected on samples formed after a long incubation period, where the fibrils were curvy and short.[36] In the work presented here, the preincorporated samples were collected after 4 h. Because there were significant differences in terms of TEM morphology, we expect the NMR structures for these two samples were also distinct.

For the preincorporated sample with POPC/POPG liposomes, incubation for 4 h led to a modest decrease in the ^{31}P CSA of ∼10%. The previous work illustrated that under the same sample condition, long incubation times resulted in a further decrease in the ^{31}P CAS to ∼30%.[36] The combination of these two observations indicated that long incubation times of the preincorporated Aβ might have disruption effects on the liposomes, presumably because of the uptake of lipids by the Aβ–lipid complex that resulted in smaller vesicles. A similar effect of the long incubation time has also been observed in the ^{31}P T_2 relaxation measurements. In the previous work, we detected the preincorporated POPC sample and the ^{31}P spectra showed two distinct peaks with relaxation times of 1.0 and 2.7 ms. In the work presented here, samples under similar conditions resulted in only one ^{31}P peak and a T_2 relaxation at ∼2.8 ms. The results suggest that the ^{31}P peak with a faster relaxation decay was induced by the long incubation time. Because a shorter T_2 time constant indicates a larger amplitude of motion and destabilization of the membrane bilayer, the difference implicated that a larger degree of membrane disruption was induced by long incubation times for the preincorporated Aβ. The major difference between the preincorporated samples with short and long incubation time was observed in the 2D spin diffusion NMR spectra. For this sample, it was clear that Aβ formed a well-folded parallel in-register β-sheet core region. However, the previous work showed that after long incubation times, the long-range cross-peak between F19 and L34 was not detected. This discrepancy suggested major structural changes during the long incubation times, and the disappearance might be attributed to either the shift in backbone registration in the hydrophobic core or the disruption of the steric zipper.[56]

Furthermore, the differences in ^{31}P T_2 relaxation rates were also observed for the preincorporated samples with distinct membrane components. A decrease in the T_2 relaxation time was observed for only POPC/POPG liposomes, not POPC liposomes or those containing 30% cholesterol. Cholesterol is known to decrease the membrane bilayer fluidity above the transition temperature, and therefore, membranes with the additional cholesterol might have less perturbation induced by the preincorporated Aβ. The difference between membranes with neutral and charged headgroups might be due to the increase in the degree of electrostatic repulsion between charged headgroups within the POPG-containing liposomes. Overall, the data suggest that the preincorporated Aβ in POPC/POPG liposomes induced certain perturbations of the membrane bilayer, which placed the ^{31}P in a more rigid chemical environment.

Rapid Formation of the Aβ–Lipid Complex in Preincorporated Samples. We observed formation of an Aβ–lipid complex after incubation for <4 h at a physiological temperature and pH value when the Aβ was preincorporated into POPC/POPG liposomes at 1:30 peptide:lipid molar ratio.

dx.doi.org/10.1021/bi501003n | *Biochemistry* 2014, 53, 7503–7514

This complex possessed a curvy and short morphology as determined by TEM. With the same incubation time and initial peptide concentration, neither the incubation of monomeric Aβ in aqueous buffer nor the external addition of Aβ to liposomes resulted in observable species with a fibrillar morphology,[36,37] indicating that the fibrillation process was greatly accelerated by the surrounding lipid molecules. Our CD results suggested that the β-sheet structure was formed during the incubation process rather than preexisting upon addition. We have noticed that the CD results were dramatically different from those of a previously published work on the preincorporated Aβ−membrane system under similar experimental conditions, where the secondary structure of Aβ was mainly random coil within a time period of 2 months.[21] However, the previous work utilized phospholipids with the transitional temperature close to the experimental (ambient) temperature, while in the work presented here, the lipids had a much lower transition temperature. Therefore, our membrane bilayer system might have dynamics stronger than those from the previous study, which seemed to affect the aggregation rates of Aβ. The NMR spectra collected upon a 4 h incubation indicated the formation of a structurally uniform species, which contains parallel in-register β-sheet domains in both the N- and C-terminal β-strand segments. In the meanwhile, there were long-range contacts between the two β-strand segments as well as the residues in the loop region. All the NMR data supported the formation of the fibrillar structure as in the case of the mature fibrils. More interestingly, we observed that the fibrillar species contained not only Aβ but also phospholipids with specific interactions between the two molecules. The phosphate headgroups were observed to be close to residues D23 and L34, and the bulk methylene groups in the lipid acyl chain were close to residues D23 and S26. Considering that D23 and L34 were not close to the β-loop-β structural motif, it is possible that there are at least two binding sites for the phospholipids. Figure 7 displays a schematic model for the process of Aβ

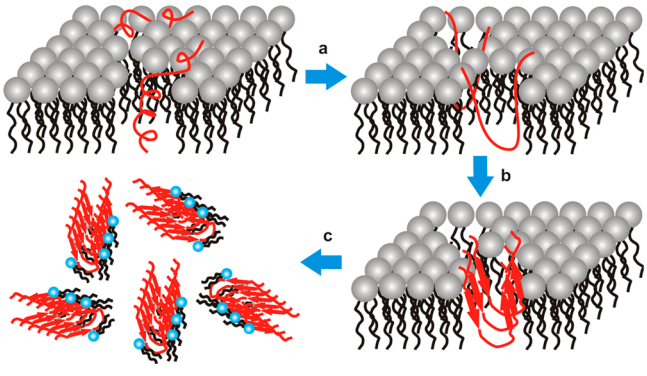

Figure 7. Cartoon models for the Aβ structural evolution in the preincorporated samples. On the basis of the NMR data, Aβ molecules formed aggregates with parallel in-register β-sheet structure in complex with lipids. The peptide might undergo structural evolution of (a) conformational change, (b) aggregation, and (c) lipid uptake.

aggregation and lipid uptake in the preincorporated sample. The initial state of binding of Aβ to the membrane bilayer was adopted from the previously published C-terminal domain of APP using solution NMR spectroscopy.[8] After enzymatic cleavage of APP, the C-terminus of Aβ was located in the hydrophobic membrane interior, which was energetically disfavored. The 40-residue Aβ sequence contains two hydrophobic regions that are composed of residues L17−A21 and A30−V40. There are three polar segments at the N-terminus, loop region, and C-terminus. The polar residues have a strong tendency to be located in the polar phospholipid headgroup region.[57] It seems that the only approach to satisfy the preferred membrane location of all segments in Aβ is to form a β-loop-β motif so that the two β-strands are located in the membrane interior and the two terminal regions and the loop regions are close to the membrane surface. This requires reorientation of the Aβ molecules by moving the charged C-terminus out of the membrane interior. In fact, the formation of such a β-loop-β motif has been reported previously in both experimental and computational simulation studies and was proposed as a precursor for the fibrillation process.[58,59] There could be multiple ways to stabilize the folded Aβ monomer. It might penetrate and span the membrane bilayer and be stabilized by oligomerization inside the bilayer, which has been previously shown in the amyloid ion channel structures by molecular dynamics simulation.[60,61] However, the channel structure was observed at a much lower peptide:lipid molar ratio compared with the conditions used in our studies. Besides, for the folded Aβ to span the entire membrane interior, its hydrophobic core region would have to cover a distance of 30−40 Å. This would require a core region with at least 20 residues, which was only observed previously in the mature Aβ fibrils. For the protofibrils with curvy morphologies, the hydrophobic core might be smaller.[18] At a high peptide:lipid ratio, the Aβ molecules are more likely to be in the proximity of themselves rather than lipids, and this will promote fibrillation. We detected a rapid and immediate ThT fluorescence enhancement, which verified the formation of fibrillar structures. Because of the aggregation, the Aβ molecules are less likely to penetrate the membrane bilayer because of the increment in the size of the polar region, and because the hydrophobic effect can be satisfied by self-association rather than insertion into membrane interiors. We have provided solid-state NMR evidence of the binding between Aβ and lipids. It is particularly interesting that the binding was residue-specific rather than random; i.e., the lipid molecules seemed to bind to the loop region (i.e., D23 and S26) rather than the two hydrophobic segments. The binding might occur through electrostatic interactions, and the loop region is composed of more polar and charged residues. However, we did not rule out the possibility that there were multiple binding sites, for instance, the N-terminus that contains mainly polar amino acids. We noticed that in the published structural model of the membrane binding domain of APP, the loop residues of Aβ are located in the interface between the polar lipid headgroups and hydrophobic acyl chains. There were significant ^{1}H chemical shift variations for residues E22, G29, and G33 in response to the changes in membrane composition, which suggested interactions between this region and membrane components.[8] Our observation that residues D23, S26, and L34 had close contact with lipids was consistent with the membrane binding sites proposed for APP, which means that the binding might occur before the formation of fibrils.

Fibrillation Pathway in Externally Added Samples. The decay curves from the ^{13}C-PITHIRDs-CT experiments reveal the strength of dipolar coupling between labeled ^{13}C nuclei, and more specifically for the singly labeled samples, the ^{13}C isotopes within the same residue from the adjacent peptide chain. In general, faster decay indicates either shorter ^{13}C−^{13}C distances or less dynamics, both of which will generate stronger

dx.doi.org/10.1021/bi501003n | Biochemistry 2014, 53, 7503−7514

dipolar coupling.[43] The combination of 2D RAD and PITHIRDs experiments suggested that residue A21 forms well-ordered β-sheet structure rapidly. Segments around A21 have been proposed to be the binding sites for the membrane surface in the model of the C-terminal domain of APP.[8] Therefore, the conformation within the segment might be restricted because of membrane binding. The C-terminal β-sheet formed with a relatively slower rate, probably after incubation for 48 h. The 2D experiments showed that the local secondary structure for A30 and L34 did not change after 24 h. Therefore, the slower PITHIRDs curves on day 2 for the methyl group of A30 and the carbonyl group of M35 were probably due to the motion of the C-terminal β-strand rather than the presence of multiple conformations with different internuclear distances. Although residue A21 seemed to have a restricted conformation and formed β-sheet quickly, the residues toward the N-terminus were more flexible. F19 possessed multiple conformations after 2 days and slowly reached conformational convergence after 4 days. The carbonyl group of V18 seemed to have the slowest rate of forming parallel in-register β-sheets among the four labeled sites. It was unclear why there is a difference in the fibrillation kinetics between V18 and A21. It might be related to the residue-specific details in the binding domain of Aβ to the membrane bilayer. It was reported that the fibrillation pathway of the islet polypeptide (IAPP) was initiated in the loop region followed by the two β-strands.[62] The mature fibril of IAPP has a structure very similar to that of the Aβ fibrils. However, the fibrillation pathways might be different for the two amyloid peptides. We should also emphasize that the presence of the membrane bilayer may affect the fibrillation process because membrane binding can provide conformational restriction to certain segments on the peptide that may facilitate or disfavor fibril formation. It was proposed previously that the interaction between amyloid peptides and membranes provided preferred orientations that might facilitate the fibrillation.[5,12] In that sense, the preincorporated Aβ molecules may have less dynamics as they were surrounded by lipids, while in the externally added case, the peptide may be only loosely associated with the membrane surface.

Insights into Membrane Disruption. Characterization of the molecular-level mechanism of membrane disruption induced by amyloid peptides remains a major challenge that prevents further understanding of the neurotoxicity of these peptides. Recent clinical studies of the anti-amyloid drugs have raised questions about the validation of the amyloid cascade hypothesis.[1−3] However, to obtain molecular-level evidence that either supports or opposes the hypothesis, it is crucial to utilize biologically relevant model systems. The initial proximity between Aβ and the membrane and the relative ratio of the peptide to lipids are important factors that have to be considered in model systems. As we have shown in this work, the Aβ peptides behave quite differently under the externally added and preincorporated conditions. For the preincorporated sample and relatively high peptide:lipid ratio, we observed the rapid formation of a complex composed of both Aβ and lipids. The formation of such a complex might involve the rapid assembly of a fibrillar core followed by elution from the membrane bilayer with lipid uptake. Therefore, the complex will induce disruption to the membrane by affecting the integrity of the bilayer structure. It was shown that Aβ could be concentrated within certain domains of the membrane such as the lipid raft.[9] Our results have suggested that at high local Aβ concentrations, the peptide might form aggregates together with phospholipids and disrupt the membrane bilayer. The externally added Aβ forms mature fibril after a long incubation time. As opposed to the preincorporated samples, we did not observe obvious membrane disruption during the initial stage of fibrillation. However, fibril formation might still have an instant interaction with the lipid bilayer because of its potential binding to the membrane. Future investigations will be performed to characterize the initial membrane binding states of Aβ, the membrane-facilitated aggregation, and the consequent Aβ−membrane interactions.

CONCLUSIONS

We reported high-resolution studies of the different Aβ aggregation pathways and the consequent membrane disruption with different initial proximities between the peptide and membrane bilayer. Different sample preparation protocols provide biologically relevant mimics for either the released Aβ or the inserted Aβ. The preincorporated sample preparation resulted in the rapid formation of a complex between Aβ aggregates and lipids, which contains a parallel in-register β-sheet core similar to the mature fibril. Formation of the complex was associated with lipid uptake and possibly membrane disruption. When Aβ was externally added to the preformed liposome, mature fibrils were produced after long incubation times. Different residues along the peptide sequence reached conformational convergence and formed β-sheet structure at different rates. In general, the segments around A21 seem to form well-ordered, parallel in-register β-sheet structure quickly. The C-terminal segments formed a parallel β-sheet before the structural convergence in the loop region and the residues located close to the N-terminus. Unlike the rapid formation of protofibrils in the preincorporated samples, the slow fibrillation process did not seem to have a significant effect on the integrity of the membrane bilayer.

ASSOCIATED CONTENT

Supporting Information

Representative static and MAS ^{31}P solid-state NMR spectra, additional fluorescence measurements, and a cartoon model to show interstrand distances in ^{13}C-PITHIRDs-CT experiments. This material is available free of charge via the Internet at http://pubs.acs.org.

AUTHOR INFORMATION

Corresponding Author

*Department of Chemistry, Binghamton University, State University of New York, Binghamton, NY 13902. E-mail: wqiang@binghamton.edu. Telephone: (607) 777-2298.

Funding

The work is supported by the Startup package from Binghamton University for W.Q. and the National Science Foundation, Major Research Instrument Foundation (NSF0922815). We are grateful for the financial support of R.D.A. by the Louis Stokes Alliances for Minority Participation (LSAMP) of the National Science Foundation (NSF).

Notes

The authors declare no competing financial interest.

■ ACKNOWLEDGMENTS

We greatly appreciate the technical support of Dr. Juergen Schulte in the NMR facility of the Department of Chemistry of Binghamton University.

■ ABBREVIATIONS

Aβ, β amyloid; AD, Alzheimer's disease; AFM, atomic force microscopy; APP, amyloid precursor protein; CD, circular dichroism; CP, cross-polarization; CSA, chemical shift anisotropy; IAPP, islet amyloid polypeptide; MAS, magic angle spinning; NMR, nuclear magnetic resonance; POPC, 1-palmitoyl-2-oleoyl-*sn*-glycero-3-phosphocholine; POPG, 1-palmitoyl-2-oleoyl-*sn*-glycero-3-phosphoglycerol; RAD, radiofrequency-assisted diffusion; REDOR, rotational echo double resonance; TEM, transmission electron microscopy; ThT, thioflavin T; TPPM, two-pulse phase modulation.

■ REFERENCES

(1) Karran, E., Mercken, M., and De Strooper, B. (2011) The amyloid cascade hypothesis for Alzheimer's disease: An appraisal for the development of therapeutics. *Nat. Rev. 10*, 698−712.

(2) Hardy, J. A., and Higgins, G. A. (1992) Alzheimer's disease: The amyloid cascade hypothesis. *Science 256*, 184−185.

(3) Tayeb, H. O., Murray, E. D., Price, B. H., and Tarazi, F. I. (2013) Bapineuzumab and solanezumab for Alzheimer's disease: Is the 'amyloid cascade hypothesis' still alive? *Expert Opin. Biol. Ther. 13*, 1075−1084.

(4) Jelinek, R., and Sheynis, T. (2010) Amyloid−membrane interaction: Experimental approaches and techniques. *Curr. Protein Pept. Sci. 11*, 372−384.

(5) Butterfield, S. M., and Lashuel, H. A. (2010) Amyloidogenic protein-membrane interactions: Mechanistic insight from model systems. *Angew. Chem. 49*, 5628−5654.

(6) Kukar, T. L., Ladd, T. B., Robertson, P., Pintchovski, S. A., Moore, B., Bann, M. A., Ren, Z., Jansen-West, K., Malphrus, K., Eggert, S., Maruyama, H., Cottrell, B. A., Das, P., Basi, G. S., Koo, E. H., and Golde, T. E. (2011) Lysine 624 of the amyloid precursor protein (APP) is a critical determinant of amyloid β peptide length: Support for a sequential model of γ-secretase imtramembrane proteolysis and regulation by the APP juxtamembrane region. *J. Biol. Chem. 286*, 39804−39812.

(7) Beel, A. J., Mobley, C. K., Kim, H. J., Tian, F., Hadziselimovic, A., Jap, B., Prestegard, J. H., and Sanders, C. R. (2008) Structural studies of the transmembrane C-terminlal domain of the amyloid precursor protein (APP): Does APP function as a cholesterol sensor? *Biochemistry 47*, 9428−9446.

(8) Barrett, P. J., Song, Y. L., Van Horn, W. D., Hustedt, E. J., Schafer, J. M., Hadziselimovic, A., Beel, A. J., and Sanders, C. R. (2012) The amyloid precursor protein has a flexible transmembrane domain and binds cholesterol. *Science 336*, 1168−1171.

(9) Mason, R. P., Jacob, R. F., Walter, M. F., Mason, P. E., Avdulov, N. A., Chochina, S. V., Igbavboa, U., and Wood, W. G. (1999) Distribution and fluidizing action of soluble and aggregated amyloid β-peptide in rat synaptic plasma membranes. *J. Biol. Chem. 275*, 18801−18807.

(10) Mason, R. P., Estermyer, J. D., Kelly, J. F., and Mason, P. E. (1996) Alzheimer's disease amyloid β peptide 25−35 is localized in the membrane hydrophobic core: X-ray diffraction analysis. *Biochem. Biophys. Res. Commun. 222*, 78−82.

(11) Hane, F., Drolle, E., Gaikward, R., Faught, E., and Leonenko, Z. (2011) Amyloid-β aggregation on model lipid membranes: An atomic force microscopy study. *Journal of Alzheimer Research 26*, 485−494.

(12) Yip, C. M., and McLaurin, J. (2001) Amyloid-β peptide assembly: A critical step in fibrillogenesis and membrane disruption. *Biophys. J. 80*, 1359−1371.

(13) Muller, W. E., Koch, S., Eckert, A., Hartmann, H., and Scheuer, K. (1995) β-Amyloid peptide decreases membrane fluidity. *Brain Res. 674*, 133−136.

(14) Peters, I., Igbaaboa, U., Schuett, T., Haidari, S., Hartig, U., Rosello, X., Boettner, S., Copanaki, E., Deller, T., Koegel, D., Wood, W. G., Mueller, W. G., and Eckert, G. P. (2009) The interaction of β-amyloid peotein with cellular membrane stimulates its own production. *Biochim. Biophys. Acta 1788*, 964−972.

(15) Eckert, G. P., Wood, W. G., and Mueller, W. E. (2010) Lipid membranes and β-amyloid: A harmful connection. *Curr. Protein Pept. Sci. 11*, 319−325.

(16) Paravastu, A. K., Leapman, R. D., Yau, W. M., and Tycko, R. (2008) Molecular structural basis for polymorphism in Alzheimer's β-amyloid fibrils. *Proc. Natl. Acad. Sci. U.S.A. 105*, 18349−18354.

(17) Petkova, A. T., Yau, W. M., and Tycko, R. (2006) Experimental constraints on quaternary structure in Alzheimer's β-amyloid fibrils. *Biochemistry 45*, 498−512.

(18) Qiang, W., Yau, W. M., Luo, Y. Q., Mattson, M. P., and Tycko, R. (2012) Antiparallel β-sheet architecture in Iowa-mutant β-amyloid fibrils. *Proc. Natl. Acad. Sci. U.S.A. 109*, 4443−4448.

(19) Petkova, A. T., Ishii, Y., Balbach, J. J., Antzutkin, O. N., Leapman, R. D., Delaglio, F., and Tycko, R. (2002) A structural model for Alzheimer's β-amyloid fibrils based on experimental constraints from solid state NMR. *Proc. Natl. Acad. Sci. U.S.A. 99*, 16742−16747.

(20) Lu, J. X., Qiang, W., Yau, W. M., Schwieters, C. D., Meredith, S. C., and Tycko, R. (2013) Molecular structure of β-amyloid fibrils in Alzheimer's disease brain tissue. *Cell 154*, 1257−1248.

(21) Bokvist, M., Lindstrom, F., Watts, A., and Grobner, G. (2004) Two types of Alzheimer's β-amyloid (1−40) peptide membrane interactions: Aggregation preventing transmembrane anchoring versus accelerated surface fibril formation. *J. Mol. Biol. 335*, 1039−1049.

(22) Williams, T. L., and Serpell, L. C. (2011) Membrane and surface interactions of Alzheimer's Aβ peptide: Insights into the mechanism of cytotoxicity. *FEBS J. 278*, 3905−3917.

(23) McLaurin, J., and Chakrabartty, A. (1997) Characterization of the interactions of Alzheimer's β-amyloid peptides with phospholipid membranes. *Eur. J. Biochem. 245*, 355−363.

(24) Lockhart, C., and Klimov, D. K. (2014) Alzheimer's Aβ 10−40 peptide binds and penetrates DMPC bilayer: An isobaric-isothermal replica exchange molecular dynamics study. *J. Phys. Chem. B 118*, 2638−2648.

(25) Lockhart, C., and Klimov, D. K. (2013) Revealing hidden helix propensity in Aβ peptides by molecular dynamics simulations. *J. Phys. Chem. B 117*, 12030−12038.

(26) Capone, R., Jang, H., Kotler, S. A., Connelly, L., Arce, F. T., Ramachandran, S., Kagan, B. L., Nussinov, R., and Lal, R. (2012) All-D-Enantiomer of β-amyloid peptide forms ion channels in lipid bilayers. *J. Chem. Theory Comput. 8*, 1143−1152.

(27) Lin, H., Bhatia, R., and Lal, R. (2001) Amyloid β protein forms ion channels: Implications for Alzheimer's disease pathophysiology. *FASEB J. 15*, 2433−2444.

(28) Quist, A., Doudevski, I., Lin, H., Azimova, R., Ng, D., Frangione, B., Kagan, B., Ghiso, J., and Lal, R. (2005) Amyloid ion channels: A common sturctural link for protein-misfolding disease. *Proc. Natl. Acad. Sci. U.S.A. 102*, 10427−10432.

(29) Connelly, L., Jang, H., Arce, F. T., Ramachandran, S., Kagan, B. L., Nussinov, R., and Lal, R. (2012) Effects of point substitutions on the structure of toxic Alzheimer's β-amyloid channels: Atomic force microscopy and molecular dymanics simulations. *Biochemistry 51*, 3031−3038.

(30) Sparr, E., Engel, M. F. M., Sakharov, D. V., Sprong, M., Jacobs, J., de Kruijff, B., Hoppener, J. W. H., and Killian, J. A. (2004) Islet amyloid polypeptide-induced membrane leakage involves uptake of lipids by forming amyloid fibers. *FEBS Lett. 577*, 117−120.

(31) Niu, Z., Zhao, W., Zhang, Z., Xiao, F., Tang, X., and Yang, J. (2014) The molecular structure of Alzheimer β-amyloid fibrils formed in the presence of phospholipid vesicles. *Angew. Chem., Int. Ed. 53*, 9294−9297.

(32) Ladiwala, A. R. A., Bhattacharya, M., Perchiacca, J. M., Cao, P., Raleigh, D. P., Abedini, A., Schmidt, A. M., Varkey, J., Langen, R., and Tessier, P. M. (2012) Rational design of potent domain antibody inhibitors of amyloid fibril assembly. *Proc. Natl. Acad. Sci. U.S.A. 109*, 19965−19970.
(33) Petrassi, H. M., Klabunde, T., Sacchettini, J., and Kelly, J. W. (2000) Structure-based design of N-phenoxazine transthyretin amyloid fibril inhibitors. *J. Am. Chem. Soc. 122*, 2178−2192.
(34) Sievers, S. A., Karanicolas, J., Chang, H. W., Zhao, A., Jiang, L., Zirafi, O., Stevens, J. T., Munch, J., Baker, D., and Eisenberg, D. (2011) Structure-based design of non-natural amino-acid inhibitors of amyloid fibril formation. *Nature 475*, 96−117.
(35) O'Brien, R. J., and Wong, P. C. (2011) Amyloid precursor protein processing and Alzheimer's disease. *Annu. Rev. Neurosci. 34*, 185−204.
(36) Qiang, W., Yau, W. M., and Schulte, J. (2014) Fibrillation of β amyloid peptides in the presence of phospholipid bilayers and the consequent membrane disruption. *Biochim. Biophys. Acta*, DOI: 10.1016/j.bbamem.2014.04.011.
(37) Qiang, W., Kelley, K., and Tycko, R. (2013) Polymorph-specific kinetics and thermodynamics of β-amyloid fibril growth. *J. Am. Chem. Soc. 135*, 6860−6871.
(38) Qiang, W., and Weliky, D. P. (2009) HIV Fusion Peptide and its corss-linkedin oligomers: Efficient synthesis, significance of the trimer in fusion activity, correlation of β strand conformation with membrane cholesterol, and proximity to lipid headgroups. *Biochemistry 48*, 289−301.
(39) Yang, R., Prorok, M., Castellino, F. J., and Weliky, D. P. (2004) A trimeric HIV-1 fusion peptide construct which does not self-associated in aqueous solution and which has 15-hold higher membrane fusion rate. *J. Am. Chem. Soc. 126*, 14722−14723.
(40) Sreerama, N., and Woody, R. W. (2004) On the analysis of membrane protein circular dichroism spectra. *Protein Sci. 13*, 100−112.
(41) Morcombe, C. R., Gaponenko, V., Byrd, R. A., and Zilm, K. W. (2004) Diluting abundant spins by isotope edited radio frequency field assisted diffusion. *J. Am. Chem. Soc. 126*, 7196−7197.
(42) Qiang, W., Sun, Y., and Weliky, D. P. (2009) A strong correlation between fusogenicity and membrane insertion depth of the HIV fusion peptide. *Proc. Natl. Acad. Sci. U.S.A. 106*, 15314−15319.
(43) Tycko, R. (2007) Symmetry-based constant-time homonuclear dipolar recoupling in solid state NMR. *J. Chem. Phys. 126*, 064506.
(44) Bak, M., Rasmussen, J. T., and Nielsen, N. C. (2000) SIMPSON: A general simulation program for solid-state NMR spectroscopy. *J. Magn. Reson. 147*, 296−330.
(45) Fonsece, A. C., Resende, R., Oliveira, C. R., and Pereira, C. M. F. (2010) Cholesterol and statins in Alzheimer's disease: Current controversies. *Exp. Neurol. 223*, 282−293.
(46) Wolozin, B. (2001) A fluid connection: Cholesterol and Aβ. *Proc. Natl. Acad. Sci. U.S.A. 98*, 5371−5373.
(47) Drechsler, A., Anderluh, G., Norton, R. S., and Separovic, F. (2010) Solid-state NMR study of membrane interactions of the pore-forming cytolysin, equinatoxin II. *Biochim. Biophys. Acta 1798*, 244−251.
(48) Bonov, B. B., Lam, Y., Anderluh, G., Watts, A., Norton, R. S., and Separovic, F. (2003) Effects of the eukaryotic pore-forming cytolysin equinotoxin II on lipid membranes and the role of sphingomyelin. *Biophys. J. 84*, 2382−2392.
(49) Chimon, S., Shalbat, M. A., Jones, C. R., Calero, D. C., Alzezi, B., and Ishii, Y. (2007) Evidence of fibril-like β sheet structures in a neurotoxic amyloid intermediate of Alzheimer's β-amyloid. *Nat. Struct. Mol. Biol. 14*, 1157−1164.
(50) Luhrs, T., Ritter, C., Adrian, M., Riek-Loher, D., Bohrmann, B., Dobeli, H., Schibert, D., and Riek, R. (2005) 3D structure of Alzheimer's amyloid-β(1−42) fibrils. *Proc. Natl. Acad. Sci. U.S.A. 102*, 17342−17347.
(51) Manolikas, T., Herrmann, T., and Meier, B. H. (2008) Protein structure determination from ^{13}C spin-diffusion solid-state NMR spectrosocpy. *J. Am. Chem. Soc. 130*, 3959−3966.
(52) Tycko, R., Sciarretta, K. L., Orgel, J. P. R. O., and Meredith, S. C. (2009) Evidence for novel β-sheet structures in Iowa mutant β-amyloid fibrils. *Biochemistry 48*, 6072−6084.
(53) Lee, C. W., and Griffin, R. G. (1989) Two-dimensional ^{1}H/^{13}C heteronuclear chemical shift correlation spectroscopy of lipid bilayer. *Biophys. J. 55*, 355−358.
(54) Mueller, K. T. (1995) Analytical solutions for the time evolution of dipolar-dephasing NMR signals. *J. Magn. Reson. 113*, 81−93.
(55) Tycko, R. (2011) Solid-state NMR studies of amyloid fibril structure. *Annu. Rev. Phys. Chem. 62*, 279−299.
(56) Sawaya, M. R., Sambashivan, S., Nelson, R., Ivanova, M. I., Sievers, S. A., Apostol, M. I., Thompson, M. J., Balbirnie, M., Wiltzius, J. J., McFarlane, H. T., Madsen, A. O., Riekel, C., and Eisenberg, D. (2007) Atomic structure of amyloid cross-β spines reveal varied steric zipper. *Nature 447*, 453−457.
(57) Bowie, J. U. (2005) Solving the membrane protein folding problem. *Nature 438*, 581−589.
(58) Lazo, N. D., Grant, M. A., Condron, M. C., Rigby, A. C., and Teplow, D. B. (2005) On the nucleation of amyloid β-protein monomer folding. *Protein Sci. 14*, 1581−1596.
(59) Baumketner, A., Bernstein, S. L., Wyttenbak, T., Bitan, G., Teplow, D. B., Bowers, M. T., and Shea, J. (2006) Amyloid β-protein monomer structure: A computational and experimental study. *Protein Sci. 15*, 420−428.
(60) Lal, R., Lin, H., and Quist, A. P. (2007) Amyloid β ion channel: 3D structure and relevance to amyloid channel paradigm. *Biochim. Biophys. Acta 1768*, 1966−1975.
(61) Jang, H., Arce, F. T., Ramachandran, S., Kagan, B. L., Lal, R., and Nussinov, R. (2014) Disordered amyloidogenic peptides may insert into the membrane and assemble into common cyclic structural motifs. *Chem. Soc. Rev. 43*, 6750−6764.
(62) Buchanan, L. E., Dunkelberger, E. B., Tran, H. Q., Cheng, P., Chiu, C., Cao, P., Raleigh, D. P., de Pablo, J. J., Nowick, J. S., and Zanni, M. T. (2013) Mechanism of IAPP amyloid fibril formation involves an intermediate with a transition β-sheet. *Proc. Natl. Acad. Sci. U.S.A. 110*, 19285−19290.